Expression of the neuropeptide SALMFamide 1 during Regeneration of the Seastar Radial Nerve Cord Following Arm Autotomy

Maria Byrne[1,2], Franca Mazzone[1], Maurice R. Elphick[3], Michael C. Thorndyke[4] and Paula Cisternas[1]

[1]School of Medical Science, University of Sydney, NSW 2006, Australia
[2]School of Life and Environmental Sciences, University of Sydney, NSW 2006, Australia
[3]School of Biological and Chemical Sciences, Queen Mary University of London, London E14NS, UK
[4]Department of Biological and Environmental Sciences – Kristineberg, University of Gothenburg Kristineberg 566 SE-451 78 Fiskebäckskil, Sweden

Correspondance:
Maria Byrne
maria.byrne@sydney.usyd.edu.au

Running title: Seastar CNS regeneration post-autotomy

Arm loss through separation at a specialised autotomy plane in echinoderms is inextricably linked to regeneration, but the link between these phenomena is poorly explored. We investigated nervous system regeneration post autotomy in the asteriid seastar *Coscinasterias muricata* focusing on the reorganisation of the radial nerve cord (RNC) into the ectoneural neuroepithelium and neuropile and the hyponeural region using antibodies to the seastar-specific neuropeptide SALMFamide-1 (S1). Parallel changes in the associated haemal and coelomic vessels were also examined. A new arm bud appeared in 3-5 days with regeneration over three weeks. At the nerve stump and in the RNC immediately behind, the haemal sinus/hyponeural coelomic compartments enlarged into a hypertrophied space filled with migratory cells that appear to be involved in wound healing and regeneration. The haemal and coelomic compartments provided a conduit for these cells to gain rapid access to the regeneration site. An increase in the number of glia-like cells, indicates the importance of these cells in regeneration. Proximal to the autotomy plane, the original RNC exhibited Wallerian-type degeneration, as seen in disorganised axons and enlarged S1-positive varicosities. The imperative to regrow lost arms quickly is reflected in the efficiency of regeneration from the autotomy plane facilitated by the rapid appearance of progenitor-like migratory cells. In parallel to its specialization for defensive arm detachment, the autotomy plane appears to be adapted to promote regeneration. This highlights the importance of examining autotomy induced regeneration in seastars as a model system to study nervous system regeneration in deuterostomes and the mechanisms involved with the massive migration of stem-like cells to facilitate rapid recovery.

1. Introduction

The Echinodermata is characterised by extraordinary regenerative powers harnessed as a mechanism for clonal reproduction and for replacement of damaged body parts [1-3]. Complete regeneration of autotomised or surgically amputated seastar arms has attracted attention for over 100 years [4-9]. Echinoderms are basal deuterostomes, and in this phylogenetic position are a model group, key to understanding the evolution of regenerative abilities and constraints as in chordate nervous system regeneration [10,11]. Although echinoderms are not cephalised, they have a well-developed central nervous system (CNS) [12]. The ectoneural portion has a distinct neuroepithelium containing neuronal cell bodies and an underlying neuropile that contains axons, analogous to the grey and white matter of the vertebrate spinal cord, respectively, as well as in the presence of radial glia as the supporting framework [12-16]. Morphogenesis of the regenerating echinoderm CNS is well-studied following surgical ablation and amputation [5-9]. In holothuroids, neural regeneration depends on proliferation of the radial glia [14]. In crinoids, a blastema of proliferative cells is formed [2]. Recovery of the asteroid RNC appears to involve morphallactic processes including direct outgrowth from the nerve stump in parallel with migration of cells to the regeneration site [5,6,9]. Local proliferation also occurs and there is evidence for the involvement of progenitor/stem cells sourced from distant proliferative sites [7].

In stellate echinoderms, autotomy is by far the commonest cause of arm loss in nature, inextricably linking autotomy and regeneration, although the relationship between these phenomena is not well explored [1,17,18]. We investigated arm regeneration in the asteriid asteroid *Coscinasterias muricata* following autotomy, with a focus on the RNC and the associated haemal system which is suggested to be a conduit for migratory cells involved in regeneration [19]. This species readily discards its arms through rupture at a specialised autotomy plane near the base of the arm which is morphologically designed to minimise tissue trauma [17,18]. Indeed, the comparatively prompt appearance of a new arm bud in *C. muricata* within days of autotomy [19], much faster than recovery following traumatic amputation in seastars [5,6,8], points to an adaptive link between autotomy and efficient regeneration, as proposed by Wilkie [17]. We explored this here in the first study of regrowth of the seastar RNC and associated tissues following autotomy. Asteroids are particularly amenable to investigation of CNS regeneration because the RNCs are located on the ectodermal surface, rather than being internalized in development as they are in the other echinoderms [12].

The echinoderm nervous system and associated neuroendocrine factors play an important role in regeneration with neuropeptides playing key roles as signalling molecules and neurotransmitters [20-23]. We used antibodies to the asteroid specific neuropeptide SALMFamide-1 (S1; GFNSALMF-NH_2) [24] to follow RNC regeneration into the differentiated architecture of the outer ectoneural neuroepithelium and neuropile and the inner hyponeural layer. This neuropeptide is widely distributed in the asteroid nervous system [6,16,25,26]. We focus on the S1-IR neurons which together with histology were used to document regeneration of the nervous system and associated haemal and coelomic vessels. Autotomy and regeneration are routine features of the biology of *C. muricata* and so we expected that arm regrowth might exhibit responses that differ from those reported following surgical amputation [9]. As all previous studies of CNS regeneration in seastars have involved amputation, the novel contribution of this study was to link nerve cord regrowth to the more natural phenomenon of autotomy, thereby addressing Wilkie's [17] hypothesis of the importance of this link. We examined the original nerve proximal to the newly growing RNC with respect to the potential for Wallerian-type (anterograde) degeneration, as occurs following axon damage in the vertebrate nervous system [27].

2. Material and methods

(a) Specimen collection and induction of autotomy and regeneration

Coscinasterias muricata (4-6 cm diam) (n = 35) collected near Sydney, Australia were induced to autotomize (figure 1a,b) and placed in individual aquaria to follow arm regeneration for 3 weeks at 18-21^{o}C. They were fed *ad libitum* with mussels and the regenerating arms photographed. Intact and regenerating arms (days 3, 5, 7, 8, 11, 14, 19 and 21 post-autotomy, n = 4) were dissected from animals relaxed in 7% $MgCl_2$ and fixed for histology and immunocytochemistry (ICC) in Bouin's fluid, which also decalcified the tissue. The tissues were wax embedded and sectioned (5 µm thick) from the tip of the regenerate to the autotomy site and ~ 300 µm into the original RNC. The sections were stained (haematoxylin and eosin – H/E or toluidine blue) or used for ICC. Glia-like cells with cell bodies dispersed among axons are a prominent morphological feature of the echinoderm CNS [5,13] and we counted these cells in random 50 μm^2 portions of intact and regenerating (day 7) RNCs (n = 4). These data were compared by Student's t-test. For scanning electron microscopy (SEM) arms were fixed in 2.5% glutaraldehyde in filtered seawater for 3 h, cut in cross section, dehydrated, critical-point-dried and viewed with a JOEL JSM-35C SEM.

(b) Immunocytochemistry

An antiserum against S1 (BLIII) [24] was used to characterise a neuropeptidergic system of the intact and regenerating RNC. Tissue sections were processed for ICC using the rabbit S1 antiserum employing 3,3'-diaminobenzidine (DAB) as substrate for peroxidase conjugated to secondary antibodies for the colour reaction. The sections were dehydrated through a graded ethanol series to 100% methanol and blocked for endogenous peroxidases in 100% methanol containing 3% hydrogen peroxide for 45 min at room temperature (RT) in a moist chamber followed by three rinses each in 100% methanol, 50% methanol in PBS, and 1xPBS. Nonspecific antibody binding was blocked with 5% goat serum in PBS containing 0.1% BSA for 30 min at RT in a moist chamber. Sections were incubated overnight at 4^{o}C in S1 antiserum diluted 1:10,000 in PBS/0.1% BSA. They were then rinsed three times in PBS and incubated in a 1:200 dilution of peroxidase conjugated goat anti-rabbit immunoglobulins in PBS/0.1% BSA for 1.5 h in a moist chamber. After a rinse in PBS for 1 hour they were incubated in DAB solution until brown staining was observed. The sections were rinsed in distilled water for 30 min and then coverslips were mounted on 1:1 PBS: glycerol. Controls included omission of 1) primary antiserum, 2) secondary antibodies, and 3) both of these (peroxidase controls) and 4) replacement of primary antiserum with preimmune rabbit serum.

3. Results

(a) Autotomy, wound closure and anatomy of arm regeneration

Arm autotomy in *Coscinasterias muricata* occurs at the arm base between the 5th and 6th ambulacral plates (n = 35) with the arm detaching as the mutable connective tissue ligaments softened (Figure 1a,b,2a). Muscle contraction seals the wound within 30 min to restore haemostasis. The wound was then sealed off by a thin layer of connective tissue (figure 1c-e).

By day 3-5 the presence of a complete epithelium over the nascent arm was evident in a small raised bump in the middle of the wound site (figure 1f). A new arm bud was evident by days 5-7 as a short (200-300 µm) projection with the terminal tube foot at the leading edge (figure 1g). The arm bud was almost transparent with the developing water vascular canal running down the middle evident. A terminal red spot marked formation of the ocellus. By days 11, 14 and 19 the arm bud was ca. 800 µm, 1.5 mm and 2.0 mm in length, respectively (figure 1h,i). New skeletal plates were evident by day 9 and new tube feet by day 14. Small spines appeared at the end of the arm during days 14-16 and the number of ocellar pigment spots increased. By day 21 the new arm ($\bar{x}$ = 3.0 mm long, SE = 0.1, n = 4) had well-developed plates, spines and tube feet (figure 1i).

(b) Differentiated radial nerve cord

The RNC extends along the oral surface between the tube feet and has the characteristic V-shaped profile of this structure in seastars (figure 2b-e). It has two regions, the outer ectoneural system and the inner hyponeural system (figure 2d-f). The ectoneural portion (100-150 µm diam) has two layers, a compact intensely basophilic outer pseudostratified neuroepithelium (30 µm diam), which includes neuronal cell bodies and support cells [see 12] and an inner neuropile (figure 2d-f). Glia-like cells were present among the axons ($\bar{x}$ = 6/50 µm^{2,} SE = 2, n = 4). Radial glia form the supporting framework in processes that extended across the neuropile [see 13] (figure 2f). The hyponeural system formed a thin layer (20 µm thick) along the inner side of the RNC (figure 2d). The haemal sinus is a connective tissue compartment forming an ill-defined structure that runs along the "V" space of the RNC in the hyponeural coelom (figure 2d-e). The radial water canal and hyponeural coelom run parallel to the RNC along the arm.

S1-immunoreactivity (IR) was conspicuous in the ectoneural system, where it was intense throughout the neuropile in small varicosity-like structures and so the IR appeared slightly granular (figure 2e). S1-positive cells were present in the neuroepithelium and were also scattered along the hyponeural layer (figure 2e).

(d) Regeneration of the radial nerve cord and associated structures

The new arm bud on day 3 had an epithelial cover and contained aggregation of cells that had the coelomocyte/phagocyte morphology (figure 2g). At the nerve stump these cells occurred where the hyponeural system, hyponeural coelom and haemal sinus would normally reside. By day 7-8 the RNC of the new arm was beginning to organise. The neuroepithelial cell bodies (figure 3a) were not as compact as in the fully differentiated state (figure 2d,e). At the regenerating RNC, and immediately behind, the space where the haemal sinus and hyponeural coelom would normally reside was hypertrophied and filled with migratory cells (~150-200 nuclei per section) (figure 3a-c). It appears that the haemal sinus/hyponeural coelomic compartments and the migratory cells that occupied these compartments became embedded in the ectoneural tissue (figure 3a-c,e,f). Glia-like cells were conspicuous in the neuropile and increased in number compared with the control (see above) RNC ($\bar{x}$ = 14/50 μm^2, SE = 2, n = 4; significant difference t-test, $p = 0.01$) (figure 3d). There was minimal S1-IR at the regeneration site and IR was irregular at the autotomy site (figure 3e,f). S1-IR in the neuropile at the RNC stump was sporadic and varicose. The original RNC proximal to the autotomy plane also had an irregular S1 staining in the ectoneural neuropile with large varicosities (figure 3g). Changes to the original RNC were evident for distance of 150-250 μm proximal from the wound site.

By day 11-14 the neuroepithelium had a pseudostratified arrangement, stacked 4-6 cells deep, but was yet to achieve the compact structure that characterises the fully formed RNC (figure 4a). The haemal sinus/hyponeural coelomic compartment remained as a core of tissue embedded in the ectoneural tissue that contained migratory cells, now less abundant (figure 4b). Glia-like cells were conspicuous in the neuropile. The neuropile contained disorganised axons and scattered S1-positive varicosities ($\bar{x}$ = 4.2 μm diam, n = 20) (figure 4d,e). The original RNC looked quite normal with H/E histology, although the neuroepithelium was not compact (figure 4c). With SI-IR in comparison, the neuropile appeared disorganised with punctate IR in large varicosities and an irregular staining pattern (figure 4f).

The regenerate attained the normal RNC profile by day 19-21, with further development of the neuroepithelium, although this layer was still not as compact as in the fully formed RNC (figure 5a). This time point also marked the first appearance of S1-IR cells in the neuroepithelium (figure 5b). In the neuropile S1-IR was more uniform, but still varicose. The hyponeural system was now a distinct layer with S1-IR cell bodies (figure 5a,b). The haemal sinus returned to its normal profile as a separate structure positioned in the now evident hyponeural coelom. Normal morphology of the

RNC behind the newly regenerated region took ca. 3 weeks, although the S1-IR in the neuropile (figure 5c) was still not as uniform as in the fully differentiated RNC (figure 2e).

4. Discussion

Asteriid seastars exhibit a great propensity for arm autotomy with detachment near the base of the arm, a feature associated with their stellate-narrow armed anatomy, close association between collagen loop strands and the skeleton and the mutable connective tissue of the autotomy plane [1, 17,18,28,29]. In contrast, seastars that do not readily autotomize their arms (e.g. *Echinaster* sp) often have a defensive strategy in a more robust body wall [30]. As the autotomy plane is designed for rapid detachment with minimal tissue trauma and promotes regeneration [17,18,29], we expected to see features associated with regeneration post autotomy that differed from arm growth following amputation [9]. Indeed, the aggregation of migratory cells in the haemal sinus/hyponeural coelom compartments does not occur in the fully differentiated arms of *C. muricata* nor is this evident in the regenerating arm following amputation in this (Mazzone, pers obs) or other seastars [5,6,9]. The presence of a new arm bud within days of autotomy shows the rapid recovery response in *C. muricata*.

The structure of the autotomy plane promotes swift sealing of vessels restoring haemostasis and wound closure through muscle contraction. The presence of migratory cells that likely have a phagocytic function at the wound site is typical of asteroids where these cells are involved in wound healing [5,6,9,10]. Migratory cells that occur in coelomic and haemal channels include immune cells that mount the first line of cellular defense in response to stress through phagocytosis and formation of multicellular aggregates that form clots [31,32].

The haemal sinus that runs along the hyponeural coelom in the normal RNC is a thin ill-defined strand of connective tissue. By contrast, in the wound healing and regeneration state, the haemal sinus/hyponeural coelom compartments were transformed into a conspicuous space filled with migratory cells. These cells were embedded in the ectoneural tissue, occluding the location where the haemal sinus, hyponeural system and the hyponeural coelom are normally found and appear to exude into the wound and the nascent arm bud. It is clear that thousands of cells migrate through the haemal/coelomic compartment to gain rapid access to the wound site. In the initial wound-healing period this appears to contribute to the invasion of phagocytic cells involved in repair. The migratory cells remained prominent throughout RNC regeneration until tissue architecture was restored into distinct ectoneural and hyponeural regions. As the RNC differentiated, the number of the migratory cells decreased. The haemal sinus and the hyponeural coelom started to return to their normal profile after day 14, coincident with the appearance of the hyponeural system.

While cell migration appears essential for arm regeneration in *C. muricata*, the identity and origin of these cells is not known, as is the case for seastar regeneration in general due to the difficulty of tracking these cells [9]. The massive influx of cells throughout the repair and regenerative phases in *C. muricata* indicates that these cells are probably a mixed population [see 7], potentially including, immune-phagocytic repair-healing cells and progenitor-like stem cells. It will be important to characterise and identify these cells with molecular markers. These cells are likely to be generated in proliferative centres proximal to the autotomy plane, but their source is not known. Wounding and arm autotomy in *A. rubens* induce cell proliferation in haemopoietic regions including the Tiedemann body, the axial organ and the coelomic epithelium, structures long-hypothesized to be the source of coelomocytes in asteroids [7,33,34]. These haemopoietic centres are candidate sources for the migratory cells in *C. muricata* regeneration.

In addition to cell migration, the increase in the number of glia-like cells during regeneration indicates that they were undergoing local proliferation and are important in neural regeneration. Glial cells in the asteroid CNS are suggested to provide 'niches' to support growth of axons in RNC regeneration [5]. In holothuroids, glial cells are the main proliferative population in the intact and injured CNS, as are their counterparts in vertebrates [14]. Dedifferentiated glial cells create a scaffold along which neuronal processes migrate to populate new area of the nerve cord in holothuroid regeneration [14]. In vertebrate development, glial cells provide a path for migration of neurons during CNS development and regeneration [36,37]. After arm amputation local proliferation of cells occurs in the neuroepithelium and around the regenerating arms of *A. rubens* and *L. hexactis* [5,6].

The intensity of S1-IR in the CNS of *C. muricata* is similar to that found in other seastars [6,16,26]. Strong neuropeptide immunoreactivity occurs throughout the echinoderm CNS [16,26,38], indicating multifunctional modes of activity for these neurochemicals. During neural regeneration there were marked changes to the distribution of S1 in the RNC proximal to the autotomy plane from its relatively homogeneous distribution in small varicosities to one that was less organised and with large varicosities. Varicosities were also more numerous, larger and more intensely stained in the regenerating regions of the RNC compared with the intact seastar RNC [6]. Ultrastuctural studies show that small varicosities are a normal feature of the asteroid RNC and are suggested to be sites of neurotransmitter release [35]. The enlarged varicosities in the regenerating RNC of *A. rubens* are probably sites of neuropeptide release and it has been postulated that the S1 neuropeptide in these structures has an active role in regeneration [6]. Accordingly, neuropeptides can act as neuromodulatory hormones in control of cell proliferation [39].

Changes in the neuropile of the original nerve cord proximal to the autotomy plane is similar to axonal injury in vertebrates where following injury to the distal end of the cell, degeneration occurs towards the anterior end of the cell (Wallerian degeneration) [27]. Injury-induced axon damage may be important in stimulating regeneration in *C. muricata* as shown in neural regeneration in other animals, a process that also involves development of varicosities along axons [11,40,41]. Motile varicosities appear characteristic of regenerating nerve fibres where they are suggested to play a role in transport of organelles and growth resources to axon terminals and as the location of microRNA expression which may be involved in recovery of vertebrate peripheral nerves after injury [11,40,41]. The function of the varicosities in seastar RNC regeneration warrants investigation.

In *C. muricata*, S1-IR cell bodies appeared in the neuroepithelium of the regenerating RNC by day 14, late in regeneration, as also for *A. rubens* [6]. This marked the return of this cell layer back towards its normal state. With conventional histology (H/E), the 3-week old regenerate RNC appeared normal. However, S1-IR was still irregular and in large varicosities. Thus, while the distinct tissue architecture of the RNC was largely restored, the neurochemistry was not. The RNC had restored the ectoneural and hyponeural layers and the associated haemal and coelomic systems indicating that it was close to the differentiated state, with the caveat that we do not know how long it would have taken for the peptidergic system to fully differentiate.

Regeneration following autotomy in *C. muricata* with a new arm bud appearing within a few days is faster than that reported for seastars following surgical amputation [5,6] and following amputation in *C. muricata* where the arm bud stage is delayed for 7-10 days (Mazzone, pers obs). This is not surprising as the autotomy plane of asteriid seastars has specialisations for breakage that minimizes trauma and damage to the body wall, skeleton and associated complex tissues [29]. Efficient regeneration post autotomy in *C. muricata* suggests that this is a natural adaptive strategy in seastars that readily discards arms. Mutable connective tissue is a specialised feature of autotomy and may also be involved with natural (not amputational) arm regeneration [17].

The process of regeneration is categorized into the process of morphallaxis, which involves cell migration and epimorphosis where new cells proliferate and differentiate into other cell types [42]. Growth of the arm bud involves extension of the RNC and haemal system and coelomic structures as the terminal tube foot becomes more distal to the autotomy site. These morphallactic processes occur in arm regeneration in other seastars [5]. Regeneration is suggested to involve extension of axon growth cones; a process associated with remodelling of the cytoskeleton [8]. The massive influx of migratory cells and the increase in the glia-like cells indicate that epimorphosis and morphallaxis are both important in arm regeneration in *C. muricata*, as in other seastars [9].

Autotomy and regeneration are fundamental aspects of echinoderm biology. For asteriid seastars, virtually all of which are apex predators, these phenomena are adaptive features that contribute to their success [43]. The imperative to regrow arms quickly is reflected in the efficiency of arm regrowth from the autotomy plane compared to amputational loss. This prompts an expectation that in parallel to being adapted to break, the autotomy plane also has adaptions to promote regeneration, perhaps in association with proliferative stem cell centres, as suggested by Wilkie [17] and seen here in the thousands of cells that promptly arrive at the regeneration site. This appears to be a key specialisation for regeneration in *C. muricata*. While our results provide an overview of the process of regeneration in *C. muricata*, the cellular and molecular mechanisms underlying regeneration remain to be explored.

The relatively rapid neural regeneration in *C. muricata* and other echinoderms, contrasts with the limited CNS regeneration capacity of the closely related Chordata. With the intense interest in stem cells in the invertebrate deuterostomes [44], particularly with respect to neural regeneration, our results highlight the importance to consider regeneration post autotomy in seastars as a fruitful model system. Neural regeneration in *C. muricata* provides an interesting system to study CNS regeneration in deuterostomes for biomedical research, especially in parallel with molecular investigations [45-46] to generate insights into the cellular and genetic mechanisms underlying neural regeneration in echinoderms.

Author’s contributions. FM conducted the research and PC assisted. All authors contributed to the manuscript. MRE and MCT generated S1 antiserum.

Competing interests. We declare we have no competing interests.

Funding supported by an ARC Grant to MB.

Data, the data are images, as provided herein.

Acknowledgements. Thanks to Clive Jeffrey and Demian Koop for technical assistance and to the reviewers for helpful comments.

References

1. Lawrence JM. Arm loss and regeneration in Asteroidea (Echinodermata). In: Scalera-Liaci L, Canicatti C. editors. *Echinoderm Research 1991*. Balkema, Rotterdam (1992) pp 39-52

2. Carnevali MDC. Regeneration in echinoderms: repair, regrowth, cloning. *Invert Surv J.*

(2006) 3:64–76

3. Allen JD, Richardson EL, Deaker D, Agüera A, Byrne M. Larval cloning in the crown-of-thorns sea star, a keystone coral predator. *Mar Ecol Prog Ser* (2019) 609:271-276

4 King HD. Regeneration in *Asterias vulgaris. Arch Entw Mech Org* (1898) 7: 351-363.

5. Mladenov PV, Bisgrove B, Aostra S, Burke RD. Mechanisms of arm tip regeneration in the sea star *Leptasterias hexactis*. *Roux Arch Dev Biol*. (1989) 198:19–28. (doi: 10.1007/BF00376366)

6. Moss C, Hunter J, Thorndyke MC. Pattern of bromodeoxyuridine incorporation and neuropeptide immunoreactivity during arm regeneration in the starfish *Asterias rubens*. *Phil Trans R Soc B*. (1998) 353:421–436. (doi: 10.1098/rstb.1998.0220)

7. Hernroth B, Farahani F, Brunborg G, Dupont S, Dejmek A, Skold H. Possibility of mixed progenitor cells in sea star arm regeneration. *J Exp Zool B(Mol Dev Evol)* (2010) 6:457–468. (doi: 10.1002/jez.b.21352)

8. Franco CF, Santos R, Coelho AV. Proteolytic events are relevant cellular responses during nervous system regeneration of the starfish *Marthasterias glacialis*. *J Proteomics* (2014) 99:1–25. (doi: 10.1016/j.jprot.2013.12.012)

9. Ben Khadra Y, Sugni M, Ferrario C, Bonasoro F, Coelho AV, Martinez P, Carnevali MDC. An integrated view of asteroid regeneration: tissues, cells and molecules. *Cell Tissue Res.* (2017) 370:13-28 (doi 10.1007/s00441-017-2589-9)

10. Ferrario C, Khadra YB, Czarkwiani A, Zakrzewski A, Martinez P, Colombo G, Bonasoro F, Candia Carnevali MC, Oliveri P, Sugnia M. Fundamental aspects of arm repair phase in two echinoderm models. *Dev Biol*. (2018) 433: 297–309. (doi 10.1016/j.ydbio.2017.09.035)

11. Wu D, Murashov A. Molecular mechanisms of peripheral nerve regeneration: emerging roles of microRNAs. *Front Physiol.* (2013) 4:55. (doi: 10.3389/fphys.2013.00055)

12. Heinzeller T, Welsch U. The echinoderm nervous system and its phylogenetic interpretation. In: Roth G, Wullimann MF. editors. *Brain Evolution and Cognition*. Wiley, New York, (2001) pp 41–7

13. Viehweg J, Naumann WW, Olsson R. Secretory radial glia in the ectoneural system of the sea star *Asterias rubens* (Echinodermata). *Acta Zool.* (1998) 79:119–131. (doi.org/10.1111/j.1463-6395.1998.tb01151.x)

14. Mashanov VS, Zueva OR, García-Arrarás JE. Radial glial cells play a key role in echinoderm neural regeneration. *BMC Biol.* (2013) 11:49. (doi: 10.1186/1741-7007-11-49)

15. Helm C, Karl A, Beckers P, Kaul-Strehlow S, Ulbright E, Kourtesis I, Kuhrt H, Hausen H, Bartolomaeus T, Reichenbach A, Bleidorn C. Early evolution of radial glial cells in Bilateria. *Proc Roy Soc B*. (2017) 284:20170743. (doi.org/10.6084/m9)

16. Byrne M, Cisternas P. Development and distribution of the peptidergic system in larval and adult *Patiriella*: comparison of the sea star bilateral and radial nervous systems. *J Comp Neurol*. (2002) 451:101-114. (doi: 10.1002/cne.10315)

17. Wilkie IC. Autotomy as a prelude to regeneration in echinoderms. *Microsc Res Tech*. (2001) 55:369–396. (doi: 10.1002/jemt.1185)

18. Wilkie IC, Griffiths GVR, Glennie SF. Morphological and physiological aspects of the autotomy plane in the aboral integument of *Asterias rubens* L. (Echinodermata). In: De Ridder C, Dubois P, LaHaye MC, Jangoux M. editors *Echinoderm Research*. Balkema, Rotterdam, (1990) pp 301–313

19. Mazzone F, Byrne M. The haemal sinus – A possible conduit for migratory cells involved in repair and regeneration of the radial nerve cord in *Coscinasterias muricata* following autotomy. In: Barker MF. editor. *Echinoderms 2000*. Balkema, Lisse (2001) pp 187-191

20. Thorndyke MC, Candia Carnevali MD. Regeneration neurohormones and growth factors in echinoderms. *Can J Zool*. (2001) 79:1171–1208. (doi: 10.1002/jemt.1192)

21. Elphick MR, Mirabeau O, Larhammar D. Evolution of neuropeptide signalling systems. *J Exp Biol.* (2018) 221. (doi:10.1242/jeb.151092)

22. Lin M, Egertova M, Zampronio CG, Jones AM, Elphick MR. Pedal peptide/orcokinin-type neuropeptide signaling in a deuterostome: the anatomy and pharmacology of starfish myorelaxant peptide in *Asterias rubens*. *J Comp Neurol.* (2017) 525:3890-3917. (doi: 10.1002/cne.24309)

23. Elphick MR SALMFamide salmagundi: The biology of a neuropeptide family in echinoderms. *Gen Comp Endocrinol.* (2014) 205: 23–35. (doi:10.1016/j.ygcen.2014.02.0

24. Elphick MR, Reeve JR Jr, Burke RD, Thorndyke MC. Isolation of the neuropeptide SALMFamide-1 from starfish using a new antiserum, *Peptides* (1991) 12:455-459.

25. Elphick MR, Newman SJ, Thorndyke MC. Distribution and action of SALMFamide neuropeptides in the starfish *Asterias rubens*. *J Exp Biol.* (1995) 198: 2519

26. Newman SJ, Elphick MR, Thorndyke MC. Tissue distribution of the SALMFamide neuropoeptides S1 and S2 in the starfish *Asterias rubens* using novel monoclonal and polyclonal antibodies. I. Nervous and locomotory systems. *Proc Biol Soc.* (1995) 261:139–145. (doi: 10.1098/rspb.1995.0128)

27. Glass DJ. Wallerian degeneration as a window to peripheral neuropathy. *J Neuro Sci*. 220:123-124. (doi:10.1016/j.jns.2004.03.010)

28. Blowes LM, Egertová M, Liu Y, Davis GR, Terrill NJ, Gupta HS, Elphick MR. Body wall structure in the starfish *Asterias rubens*. *J Anat.* (2017) 231:325-341. (doi: 10.1111/joa.12646)

29. Marrs J, Wilkie IC, Sköld M, Maclaren WM, McKenzie JD. Size-related aspects of arm damage, tissue mechanics, and autotomy in the starfish *Asterias rubens*. *Mar Biol.* (2000) 137:59–70. (doi.org/10.1007/s002270000)

30. O'Neill P. Structure and mechanics of starfish body wall. *J Exp Biol.* (1989) 147:53-89

31. Pinsino A, Thorndyke MC, Matranga V. Coelomocytes and posttraumatic response in the common sea star *Asterias rubens*. *Cell Stress Chaperones* (2007) 12:331–341.

32. Gorshkov AN, Blinova MI, Pinaev GP. Ultrastructure of coelomic epithelium and coelomocytes of the starfish *Asterias rubens* L. in norm and after wounding. *Cell Tissue Biol.* (2009) 3:477–490

33. Vanden Bosche JP, Jangoux, M. Epithelial origin of starfish coelomocytes. *Nature* (1976) 261:227-228. (doi :10.1038/261227a0)

34. Holm K, Dupont S, Sköld H, Stenius A, Thorndyke M, Hernroth B. Induced cell proliferation in putative haematopoietic tissues of the sea star, *Asterias rubens* (L.). *J Exp Biol.* (2008) 211:2551–2558. (doi:10.1242/jeb.018507)

35. Cobb JLS. The significance of the radial nerve cords in asteroids and echinoids. *Z Zellforsch*. (1970) 108:457-474.

36. Ferretti P. Is there a relationship between adult neurogenesis and neuron generation following injury across evolution? *Eur J Neurosci*. (2011) 34: 951-962. (doi: 10.1111/j.1460-9568.2011.07833.x)

37. Morrens J, Van Den Broeck W, Kempermann G. 2012. Glial cells in adult neurogenesis. *Glia* 60:159-174

38. Inoue M, Birenheide R, Koizumi O, Kobayakawa Y, Muneoka Y, Motokawa T. Localization of the neuropeptide NGIWYamide in the holothurian nervous system and its effects on muscular contraction. *Proc Royal Soc B.* (1999). 266: 993-993. (doi: 10.1098/rspb.1999.0735)

39. Zachary I, Wöll PJ, Rozengurt E. 1987. A role for neuropeptides in the control of cell proliferation. *Devp Biol*.124: 295-308

40. Koenig E, Kinsman S, Repasky E, Sultz L. Rapid mobility of mobile varicosities and inclusions containing a-spectrin, actin, calmodulin in regenerating axons *in vivo*. *J Neurosci*. (1985) 5: 715-729. (doi.org/10.1523/JNEUROSCI.05-03-00715.1985)

41. Malkinson G, Spira A. Clustering of excess growth resources within leading growth cones underlies the recurrent "deposition" of varicosities along developing neurites. *Exp Neurol.* (2010) 225:140-153. (doi: 10.1016/j.expneurol.2010.06.005)

42. Morgan TH. Experimental studies of the regeneration of *Planaria maculate*. *Arch Entw mech Org*. (1898) 7: 364-397

43. Lawrence JM, Byrne M, Harris L, Keegan B, Freeman S, Cowell BC. Sublethal predation in *Asterias amurensis* (eastern Bering Sea and southwestern Pacific), *Asterias rubens* (northeastern Atlantic Ocean) and *Asterias vulgaris* and *Asterias forbesi* (northwestern Atlantic Ocean) (Echinodermata: Asteroidea). *Vie et Milieu* (1999) 49: 69-73.

44. Candia Carnevali MD, Thorndyke MC, Matranga V. Regenerating echinoderms; a promise to understand stem cells potential. In: Rinkevich B, Matranga V, editors. *Stem Cells in Marine Organisms.* Springer, Heidelberg (2009) pp 165–186.

45. Thorndyke MC, Chen WC, Beesley PW, Patruno M. Molecular approach to echinoderm regeneration. *Microsc Res Tech*. (2001) 55: 474– 485.

46. Gabre JL, Martinez P, Sköld HN, Ortega-Martinez O, Abril JF. The coelomic epithelium transcriptome from a clonal sea star *Coscinasterias muricata*. *Marine Genomics* (2015) 24: 245-248. (doi.org/10.1016/j.margen.2015.07.010)

Figure legends

Figure 1. Arm autotomy and regeneration in *C. muricata*. (a-b) Holding the arm induces autotomy near the base. (c-e) Muscle contraction closes the opening as the oral and aboral body walls meet within 30 min (arrows). (f) Day 5 post-autotomy, regenerating arm is a small growth covered by epithelium (arrow). (g) Day 7, arm bud and terminal tube foot (ttf). (h) Day14, arm bud with the water vascular canal (wvs), terminal tube foot (ttf) and red pigment in the developing ocellus. (i) Day 21, pairs of tube feet (tf), spines (s) and ocellus (arrow) are evident. g, gonad; o, ossicle. Scale bars (A,B) 5 cm (C-E) 1 mm (F,G,I) 100μm (H) 150μm

Figure 2. (a-b) Schematic and histology cross sections (b,f, toluidine blue; d,g. H/E; e, S1-IR). (a) Autotomy occurs between the 5th and 6th ambulacral plates. The radial nerve (rnc) runs along the oral surface, external to these plates. The box around the arm shows the location of the histology and SEM cross sections in (b) and (c) where the nerve runs along the body surface between the tube feet (tf) and oral to the ambulacral plates (ap). (d) Cross section of the radial nerve showing the ectoneural neuropile (ec) and compact neuroepithelial cell body layer (arrow), the hyponeural system (hn) and the strand-like haemal sinus (hs) running along the hyponeural coelom (hnc). (e) S1-IR in the neuropile is relatively homogeneous. S1-IR cells are present (arrow) in the neuroepithelium and hyponeural (hn) system. (f) Ectoneural system with supporting processes from radial glia (arrow) and scattered glia-like (g) cells among axons. (g) Regenerating arm on day 5 has a complete epithelial covering (arrow) and an aggregation of migratory cells (mc) at the wound site. a, ampulla; gon, gonad; pc, pyloric caeca. Scale bars (a) 500 µm (c) 750 µm (c,e) 100 µm (f) 10 µm (g) 50 µm

Figure 3. Day 8 post-autotomy (a) Cross-section of the RNC ~ 50 µm proximal to autotomy plane showing the hypertrophied haemal sinus/hyponeural coelom compartment filled with migratory cells (mc) embedded in ectoneural (ec) tissue. The neuroepithelium is less compact than in the fully formed RNC. (b) Section of RNC further proximal to the autotomy plane. (c) Migratory cells in the haemal sinus/hyponeural coelom compartment (d) Glia-like cells (e) RNC showing large compartment filled with cells (arrow) and no specific S1-IR. (f) Section of RNC at the autotomy site showing the hypertrophied haemal sinus/hyponeural coelom compartment (hs) and disorganized axons and varicose S1-IR. (g) The original RNC appears disorganized and contains varicose S1-IR, but the haemal sinus and hyponeural coelom (hnc) appear normal. gc, glia-like cells; wvs, water vascular system. Scale bars (a,b) 50 µm (c,d) 20 µm (e-g) 100 µm.

Figure 4. Day 14 post-autotomy. (a) Cross-section of the RNC distal to the autotomy plane. The haemal sinus/hyponeural coelom compartment (*) is still hypertrophied but has reduced in size and has fewer migratory cells (mc). There is no evidence of the hyponeural layer. In the ectoneural layer (ec) the neuroepithelial cell body layer is not compact (arrow and insert). (b) Migratory cells in the haemal sinus/hyponeural coelom compartment. (c) In the RNC proximal to the autotomy site the hyponeural (hn) layer and sinus (hnc) are evident. The neuroepithelium (arrow) is not compact. (d) RNC immediately proximal to the autotomy site, the neuropile appears disorganized with scattered S1-IR varicosities (v). (e) Varicosities (f) The original RNC still lacks the normal S1-IR. The haemal sinus (hs) appears normal and the hyponeural system (hn) and coelom (hnc) are evident. gc, glia-like cells; wvs, water vascular system. Scale bars (a,c,d-f) 60 µm (a insert) 20 µm (b) 20 µm (e) 10 µm.

Figure 5. Day 19 post-autotomy. (a) The neuroepithelium its distinct but is still less compact than in the fully differentiated state (compare with Figure 2a). The haemal sinus (hs) has returned to its normal profile and the hyponeural system (hn) and coelom (hnc) are evident. Coelomocytes are present in the water vascular system (wvs). (b) With S1-IR, the ectoneural region is still developing, but S1-IR cell bodies are again present in the neuroepithelium (arrowheads). The hyponeural system (hn) is present. (c) In the RNC proximal to the autotomy plane the S1-IR is closer to normal with IR cell bodies in the neuroepithelium (arrowheads) and in the hyponeural (hn) layer. Scale bars (a-c) 80 µm.

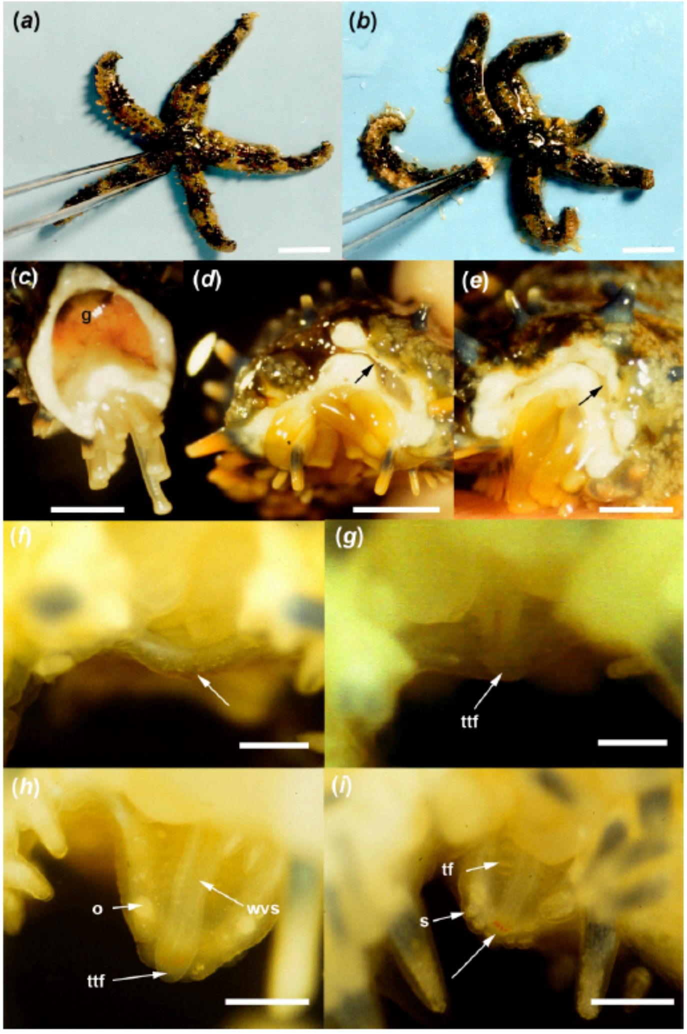

Figure 1. Arm autotomy and regeneration in C. muricata. (a-b) Holding the arm induces autotomy near the base. (c-e) Muscle contraction closes the opening as the oral and aboral body walls meet within 30 min (arrows). (f) Day 5 post-autotomy, regenerating arm is a small growth covered by epithelium (arrow). (g) Day 7, arm bud and terminal tube foot (ttf). (h) Day14, arm bud with the water vascular canal (wvs), terminal tube foot (ttf) and red pigment in the developing ocellus. (i) Day 21, pairs of tube feet (tf), spines (s) and ocellus (arrow) are evident. g, gonad; o, ossicle. Scale bars (A,B) 5 cm (C-E) 1 mm (F,G,I) 100μm (H) 150μm

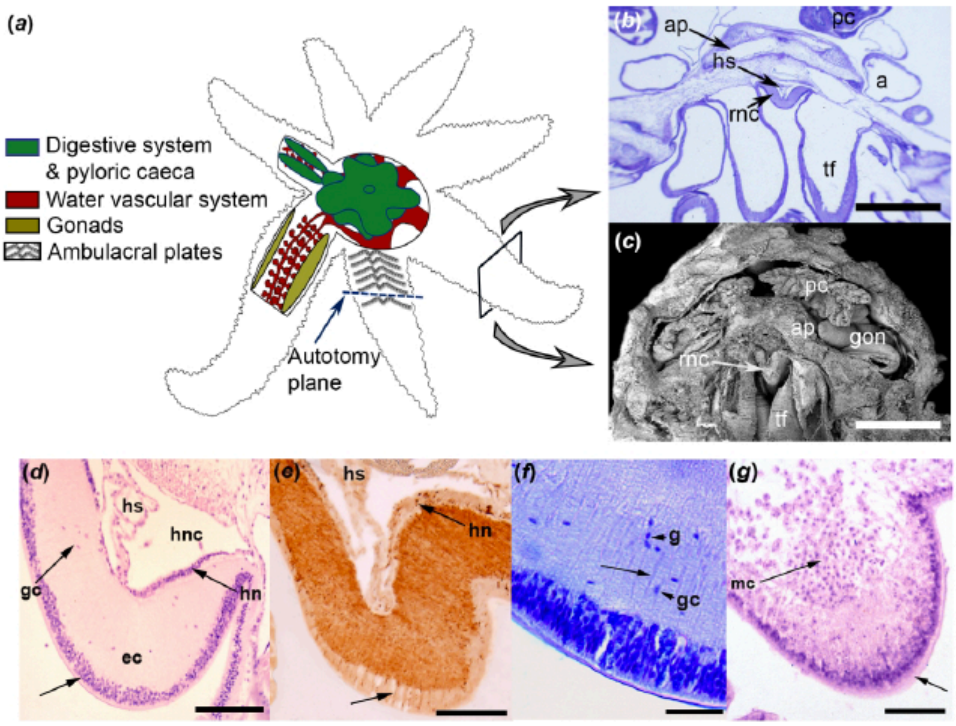

Figure 2. (a-b) Schematic and histology cross sections (b,f, toluidine blue; d,g. H/E; e, S1-IR). (a) Autotomy occurs between the 5th and 6th ambulacral plates. The radial nerve (rnc) runs along the oral surface, external to these plates. The box around the arm shows the location of the histology and SEM cross sections in (b) and (c) where the nerve runs along the body surface between the tube feet (tf) and oral to the ambulacral plates (ap). (d) Cross section of the radial nerve showing the ectoneural neuropile (ec) and compact neuroepithelial cell body layer (arrow), the hyponeural system (hn) and the strand-like haemal sinus (hs) running along the hyponeural coelom (hnc). (e) S1-IR in the neuropile is relatively homogeneous. S1-IR cells are present (arrow) in the neuroepithelium and hyponeural (hn) system. (f) Ectoneural system with supporting processes from radial glia (arrow) and scattered glia-like (g) cells among axons. (g) Regenerating arm on day 5 has a complete epithelial covering (arrow) and an aggregation of migratory cells (mc) at the wound site. a, ampulla; gon, gonad; pc, pyloric caeca. Scale bars (a) 500 µm (c) 750 µm (c,e) 100 µm (f) 10 µm (g) 50 µm

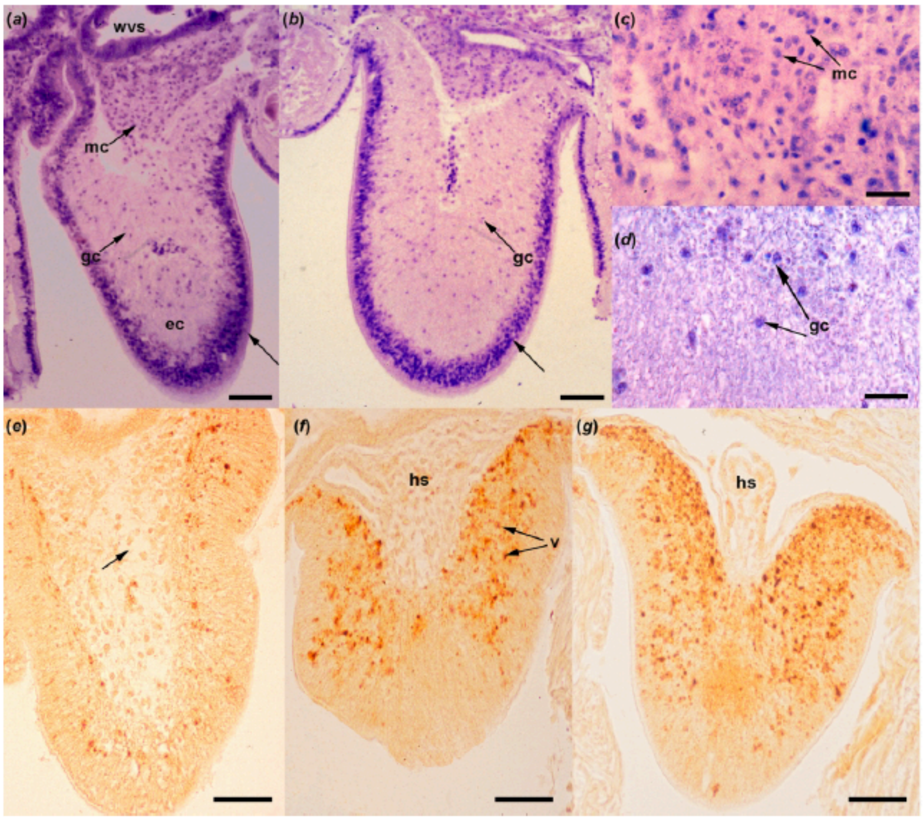

Figure 3. Day 8 post-autotomy (a) Cross-section of the RNC ~ 50 µm proximal to autotomy plane showing the hypertrophied haemal sinus/hyponeural coelom compartment filled with migratory cells (mc) embedded in ectoneural (ec) tissue. The neuroepithelium is less compact than in the fully formed RNC. (b) Section of RNC further proximal to the autotomy plane. (c) Migratory cells in the haemal sinus/hyponeural coelom compartment (d) Glia-like cells (e) RNC showing large compartment filled with cells (arrow) and no specific S1-IR. (f) Section of RNC at the autotomy site showing the hypertrophied haemal sinus/hyponeural coelom compartment (hs) and disorganized axons and varicose S1-IR. (g) The original RNC appears disorganized and contains varicose S1-IR, but the haemal sinus and hyponeural coelom (hnc) appear normal. gc, glia-like cells; wvs, water vascular system. Scale bars (a,b) 50 µm (c,d) 20 µm (e-g) 100 µm.

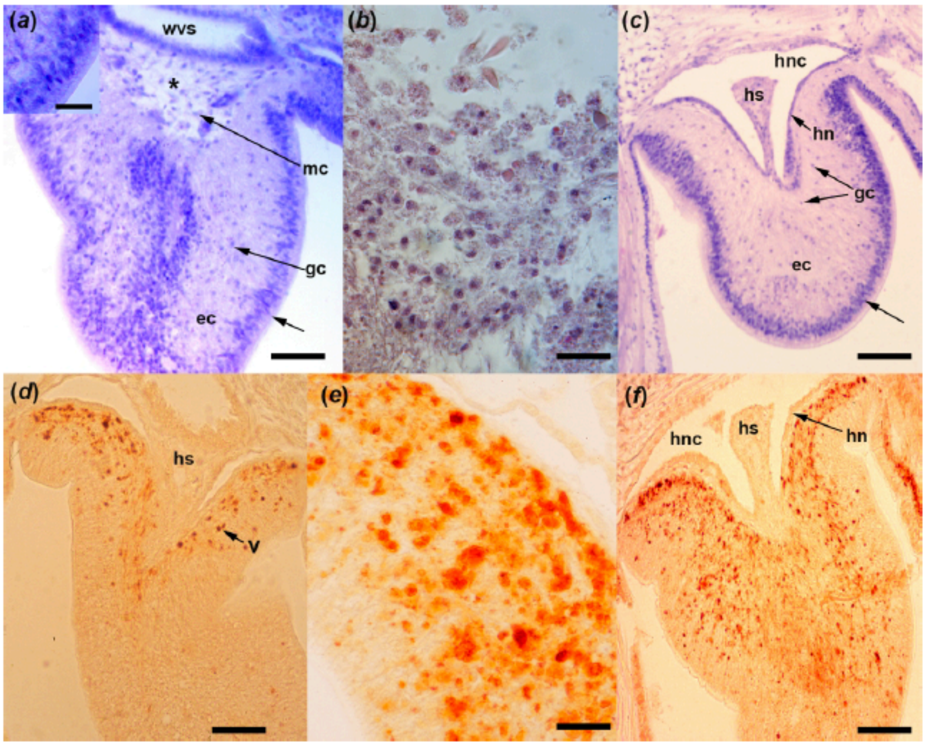

Figure 4. Day 14 post-autotomy. (a) Cross-section of the RNC distal to the autotomy plane. The haemal sinus/hyponeural coelom compartment (*) is still hypertrophied but has reduced in size and has fewer migratory cells (mc). There is no evidence of the hyponeural layer. In the ectoneural layer (ec) the neuroepithelial cell body layer is not compact (arrow and insert). (b) Migratory cells in the haemal sinus/hyponeural coelom compartment. (c) In the RNC proximal to the autotomy site the hyponeural (hn) layer and sinus (hnc) are evident. The neuroepithelium (arrow) is not compact. (d) RNC immediately proximal to the autotomy site, the neuropile appears disorganized with scattered S1-IR varicosities (v). (e) Varicosities (f) The original RNC still lacks the normal S1-IR. The haemal sinus (hs) appears normal and the hyponeural system (hn) and coelom (hnc) are evident. gc, glia-like cells; wvs, water vascular system. Scale bars (a,c,d-f) 60 µm (a insert) 20 µm (b) 20 µm (e) 10 µm.

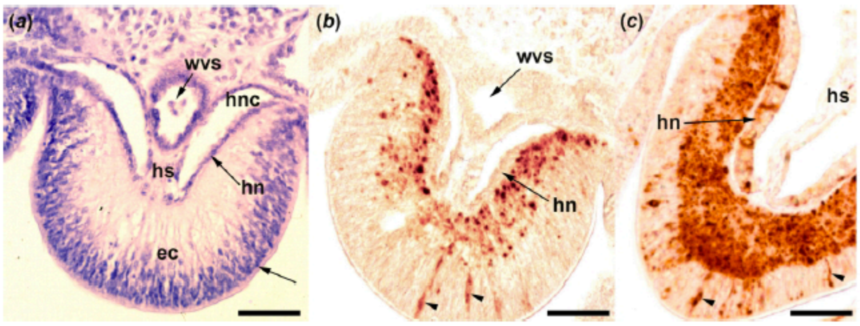

Figure 5. Day 19 post-autotomy. (a) The neuroepithelium its distinct but is still less compact than in the fully differentiated state (compare with Figure 2a). The haemal sinus (hs) has returned to its normal profile and the hyponeural system (hn) and coelom (hnc) are evident. Coelomocytes are present in the water vascular system (wvs). (b) With S1-IR, the ectoneural region is still developing, but S1-IR cell bodies are again present in the neuroepithelium (arrowheads). The hyponeural system (hn) is present. (c) In the RNC proximal to the autotomy plane the S1-IR is closer to normal with IR cell bodies in the neuroepithelium (arrowheads) and in the hyponeural (hn) layer. Scale bars (a-c) 80 µm.